

Article

UWB Positioning Algorithm Based on Fuzzy Inference and Adaptive Anti-NLOS Kalman Filtering

Junkang Wu ¹, Zuqiong Zhang ², Shenglan Zhang ¹, Zhenwu Kuang ¹ and Lieping Zhang ^{1,*} 

¹ College of Mechanical and Control Engineering, Guilin University of Technology, Guilin 51004, China; jkmexpic@163.com (J.W.); zsl@glut.edu.cn (S.Z.); kuangzw123@163.com (Z.K.)

² Network and Information Center, Guilin University of Technology, Guilin 51004, China; zzq@glut.edu.cn

* Correspondence: zlp_gx_gl@163.com; Tel.: +86-0773-3871728

Abstract: To reduce the influence of non-line-of-sight (NLOS) errors in the ultra-wideband (UWB) positioning process, a UWB positioning algorithm based on fuzzy inference and adaptive anti-NLOS Kalman filtering (KF) was proposed in this paper. First of all, the NLOS errors of the channel impulse response (CIR) signal characteristics were estimated by the fuzzy inference algorithm and then initially mitigated. Next, an adaptive anti-NLOS KF algorithm was developed to perform a second mitigation on the ranging errors after mitigation of the NLOS errors with the fuzzy inference, thereby further raising the range estimation accuracy. At last, the range estimation information after error mitigation was taken as the ranging information of the LS positioning algorithm for target localization. In the static positioning experiment, the probability of producing an error range of less than 19.1 cm with the positioning algorithm combining fuzzy inference with adaptive anti-NLOS KF was 0.93, which was much better than the positioning algorithm based on fuzzy inference and the adaptive anti-NLOS KF positioning algorithm. In the dynamic positioning experiment, compared with the adaptive anti-NLOS KF positioning algorithm, the RMSE was reduced by 43.31% in the overall positioning. Furthermore, compared with those of the positioning algorithm based on fuzzy inference, the RMSEs in overall positioning were lowered by 12.89%. The positioning accuracy was improved significantly.

Keywords: ultra-wideband positioning; non-line-of-sight; fuzzy inference; self-adaption; Kalman filter



Citation: Wu, J.; Zhang, Z.; Zhang, S.; Kuang, Z.; Zhang, L. UWB Positioning Algorithm Based on Fuzzy Inference and Adaptive Anti-NLOS Kalman Filtering. *Appl. Sci.* **2022**, *12*, 6183. <https://doi.org/10.3390/app12126183>

Academic Editor: Mirko Reguzzoni

Received: 10 May 2022

Accepted: 16 June 2022

Published: 17 June 2022

Publisher's Note: MDPI stays neutral with regard to jurisdictional claims in published maps and institutional affiliations.



Copyright: © 2022 by the authors. Licensee MDPI, Basel, Switzerland. This article is an open access article distributed under the terms and conditions of the Creative Commons Attribution (CC BY) license (<https://creativecommons.org/licenses/by/4.0/>).

1. Introduction

Under the influences of such factors as the blockage of buildings and the complexity of environments, the traditional outdoor global positioning system (GPS) satellite positioning technology is becoming unable to meet the requirements of indoor and outdoor positioning due to great positioning errors [1]. Compared with Wi-Fi, radio frequency identification, ultrasound, Bluetooth and other positioning technologies, ultra-wideband (UWB)-based positioning technology has many advantages, including centimeter-level positioning accuracy, good multi-path resistance, preferable resistance against the interference of other electronic signals from complex environments and strong penetrability [2,3], which not only endow it with high reliability but also facilitate the collection of dynamic data and real-time positioning of moving objects in complex environments [4]. The emergence of the fifth-generation mobile communication technology (5G) provides a new idea for high-precision indoor positioning. However, 5G indoor positioning technology is still immature. In addition, since the UWB frequency band and the 5G frequency band are partially shared, the UWB signal will severely impact the demodulation of the 5G signal [5].

Given the complexity of the actual positioning environment, non-line-of-sight (NLOS) errors, multi-path errors, clock drift errors and errors caused by antenna delay tend to occur in the UWB positioning process [6], among which the NLOS errors are the primary type, having a significant influence on positioning accuracy. In this context, the recognition and

mitigation of NLOS errors have become hot topics in the research on UWB positioning [7,8]. The existing methods for handling the NLOS errors mainly include [9,10]: (1) realizing integrated UWB positioning by adding hardware other than UWB, (2) identifying and mitigating the NLOS errors by virtue of filtering algorithms, (3) mitigating the NLOS errors with the positioning algorithm based on convex optimization and (4) identifying and mitigating the NLOS errors based on the channel impulse response (CIR) signal characteristics. Tian et al. [11] proposed a UWB/INS integrated location method based on an improved robust Kalman filter and support vector regression (SVR). The robust Kalman filter (RKF) is improved, and the enhanced IGG3 weight function is used to modify the innovation piecewise to reduce the influence of abnormal measurement information on the filtering result. Hu Q et al. [12] put forward a UWB-GPS combined positioning scheme, in which filtering is achieved with plane coordinates, speed and azimuth angle as observation vectors, thus improving the positioning accuracy. Zhang [13] proposed a Wi-Fi/UWB combined positioning algorithm. The algorithm first uses the ultra-wideband ranging value to filter the Wi-Fi fingerprint points. After the matching and positioning, the positioning result is added to the neighbor set as a new neighbor. The algorithm finds the nearest neighbor to the UWB base station among these neighbors and uses the position coordinates corresponding to this neighbor as the final positioning result. Moreover, by combining the inertial measurement unit and UWB, Liang Y [14] proposed an indoor positioning method that applies UWB ranging and inertial navigation fusion. A tightly coupled Kalman filter was adopted, where UWB ranging values were taken as the extended Kalman filter observation quantity, the position and attitude of the inertial navigation were taken as the extended Kalman filter prediction value, and UWB ranging values were used to constantly correct the position and attitude data of the inertial navigation solution. Zhang et al. [15] applied the KF algorithm to study the change rules in residual errors in both LOS and NLOS indoor environments. Moreover, an appropriate threshold was set and compared with the real-time residual error of ranging to identify and mitigate the NLOS errors. Liu T et al. [16] established the robust factor identification using the KF innovation vector and the threshold in the LOS environment, which is utilized to identify the NLOS errors and attenuate the influences of NLOS ranging errors and abnormal ranging values. Meanwhile, the positioning accuracy is improved by real-time estimation of system noise using the Sage–Husa filtering. Based on LOS/NLOS scene recognition, Huang et al. [17] proposed a TDOA location algorithm based on particle filter and maximum likelihood. Firstly, the approximate maximum likelihood TDOA algorithm was used to obtain a preliminary location result without distinguishing between LOS and NLOS scenes; then, the preliminary results were corrected with particle filter to reduce the increase in positioning error and inconsistency of positioning results caused by LOS and NLOS scene switching. In addition, Chen H et al. [18] introduced the “balance parameter” related to NLOS errors and proposed a new robust weighted LS problem with the target position and the NLOS balance parameter as the estimation variables. For the identification of the UWB channel state, V. Barral et al. [19] designed a statistical model by incorporating the RSSI of CIR signals and root mean square (RMS) delay characteristics. Furthermore, Marano et al. [20] developed a machine-learning model for an LS support vector machine based on the CIR channel characteristics, which can not only judge NLOS errors but also reduce the ranging errors resulting from NLOS errors. However, the algorithm accomplishes the identification and mitigation of NLOS errors in two steps, thus increasing its overall complexity. To increase the ranging accuracy, Yang [21] put forward a machine-learning method for NLOS error mitigation with low complexity based on a sparse pseudo-input Gaussian process.

Among the above methods, adding hardware for integrated positioning can improve the positioning accuracy, but such method undoubtedly increases the total cost of the positioning system and the cost of the data fusion algorithm. Given the possible influence of NLOS errors on the measured range information, the methods based on ranging estimation will have a less favorable effect on identifying and mitigating NLOS errors. Though the

machine-learning-based algorithms have the best effect on NLOS error identification and mitigation, they are not suitable for occasions with strong timeliness due to their high complexity. As the fuzzy inference algorithms possess the characteristics where no statistical model construction and data training are needed and given their high operating speed, they can mitigate the NLOS and LOS errors and improve the positioning accuracy in the case of estimating ranging errors of CIR signal characteristics, conforming to the needs of UWB node positioning [22]. The anti-NLOS KF algorithm can conduct smoothing filtering on the data and realize identification and mitigation of NLOS errors, thus effectively weakening the influence of ranging errors on positioning during UWB mobile node positioning and improving the positioning accuracy [23,24]. Based on the advantages of these two algorithms, a UWB positioning algorithm combining the fuzzy inference for NLOS error mitigation with adaptive anti-NLOS KF was proposed in this paper. In this algorithm, a fuzzy inference system of the ranging errors was first established using the changes in RSSI, first path power level (FPPL) and rise time (RT) characteristics of the CIR signals collected via ranging, and the ranging errors were initially mitigated by the fuzzy inference method. Then, the adaptive anti-NLOS KF algorithm was employed to process the range data after fuzzy inference, and the triple innovation variance was compared with the innovation to identify the NLOS errors. Moreover, the value of the innovation correction factor was automatically adjusted according to the changes in differences between innovation and innovation variance, so as to conduct second mitigation for the NLOS errors after fuzzy inference. Ultimately, the final estimated range information was substituted into the LS positioning algorithm for node positioning.

2. A Ranging Error Mitigation Algorithm for CIR Signal Characteristics Based on Fuzzy Inference

2.1. Theory of the Algorithm

The ranging errors mitigation algorithm for CIR signal characteristics based on fuzzy inference estimates the ranging errors in accordance with the changes in CIR signal characteristics. The commonly used standard CIR signal characteristics of UWB include total energy, maximum amplitude, normalized strongest path, signal-to-noise ratio, RT, average excess delay, RMS delay and kurtosis [25]. However, the level of standard implementation varies with UWB hardware manufacturers, so the actual UWB hardware should be considered together during the selection of CIR signal characteristics. In this paper, three CIR signal characteristics (RSSI, FPPL and RT) provided by the DWM1000 hardware were adopted in the ranging errors mitigation algorithm for CIR signal characteristics based on fuzzy inference.

RSSI is a signal characteristic possessed by almost all radio equipment, including DWM1000. The energy of the received signal reflects the average level of received power, which is closely correlated with the total energy characteristics in standard CIR signals. Therefore, RSSI is usually replaced by the received energy. The calculation formula of RSSI officially provided by DWM1000 is as follows:

$$RSSI = 10 \times \log_{10} \left(\frac{C \times 2^{17}}{N^2} \right) - A \quad (1)$$

where C is the power value of CIR, A represents the constant of the pulse repetition frequency, and N stands for the cumulative count value of the synchronization code.

The FPPL, officially given by DWM1000, was utilized to calculate the power estimation of the earliest first path signal arriving at the receiver. Since the discrete value of the CIR signals was obtained by sampling the wireless point signals at the time of reception, the FPPL was estimated by means of three sampling amplitudes of CIR signals that were first collected by DWM1000, which were calculated using the formula below:

$$FPPL = 10 \times \log_{10} \left(\frac{F_1^2 + F_2^2 + F_3^2}{N^2} \right) - A \quad (2)$$

where F_1 , F_2 and F_3 mean the first three sampling amplitudes of CIR signals, respectively.

RT referred to the difference between the time of the first sampling point on the first path and the time of the sampling point with the maximum amplitude, which was calculated according to the following formula:

$$RT = t_{F_{\max}} - t_{F_1} \quad (3)$$

where F_{\max} is the maximum amplitude among all the sampling points of the CIR signals, and t_{F_1} represents the sampling time of the first sampling amplitude F_1 on the first path, which can be read through the officially designated register.

The RSSI, FPPL and RT characteristics of the CIR signals reflected the severity of NLOS conditions at different levels. Specifically, the RSSI indicates the severity of NLOS in general and can be effectively classified, while FPPL and RT embody small changes in NLOS. Hence, the CIR signal characteristics can be used to mitigate the ranging errors.

2.2. Implementation of the Fuzzy Inference System

2.2.1. Selection of Structure and Membership Function of the Fuzzy Inference System

In this paper, the Mamdani fuzzy system model [26] shown in Figure 1 was adopted. Firstly, the RSSI, FPPL and RT characteristic data of the CIR signals collected by the UWB hardware were converted into fuzzy variables available for fuzzy inference through fuzzification, and then, the necessary variable of ranging errors was obtained via fuzzy inference. Finally, the fuzzy variable in the form of discourse domain was transformed by de-fuzzification into an estimated value of the ranging errors. The deviation probability distribution of the RSSI, FPPL, RT and ranging errors of CIR signals were basically in line with the Gaussian distribution. Here, the Gaussian membership function was selected for inputting the RSSI, FPPL and RT and outputting the ranging errors.

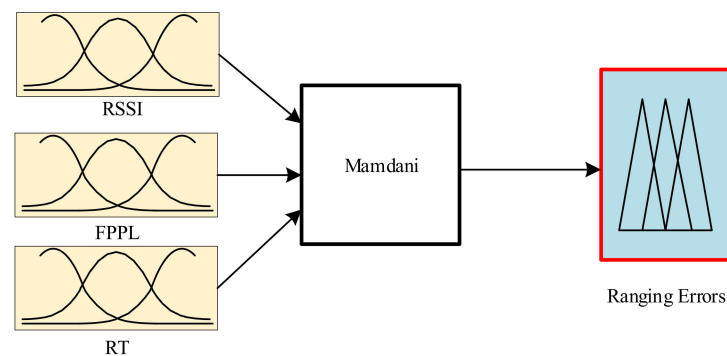


Figure 1. Structure of the fuzzy system for mitigating ranging errors based on the Mamdani model.

2.2.2. Determination of Fuzzy Sets and Fuzzy Rules

In the present study, the commonly used indoor objects, such as iron plates, wooden boards and the human body, were used as the obstacles to construct the fuzzy sets and fuzzy rules for the CIR signal characteristics of UWB and the NLOS errors. The experimental scene of the testing environment is depicted in Figure 2. The experimental processes to establish the relationship between the CIR signal characteristics of UWB and the ranging errors in an NLOS environment are set as follows: (1) The base station node was fixed at a specific position, and the tag node was placed 0.5 m away from the base station; (2) An obstacle was placed 10 cm away from the base station node to collect the signal characteristic data 500 times; (3) The distance between the obstacle and the base station node was increased by 20 cm after each measurement of a group of data, followed by 500 times of signal characteristic data collection; (4) The obstacle was moved in the above-mentioned method until it could not be placed between the tag node and the base station node; (5) The distance between the tag node and the base station node was increased by 0.5 m, and the previous procedures were repeated until this distance reached 3 m.

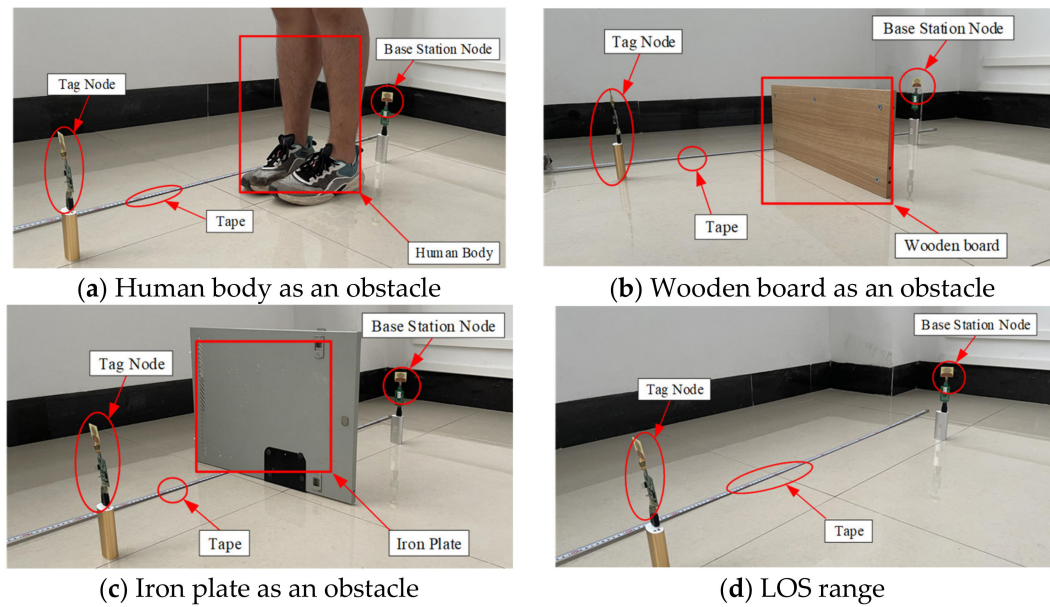


Figure 2. Specific testing environment.

The experimental scene for exploring the relationship between the CIR signal characteristics of UWB and the ranging errors in the LOS environment was basically consistent with that in the NLOS environment, except that the former had no obstacles in the middle. The experimental processes are set below: (1) The base station node was fixed at a specific position, while the tag node was placed 0.5 m away from it, and the signal characteristic data were collected 500 times at this position; (2) The position of the tag node was changed to increase the distance by 0.5 m, the corresponding testing was conducted, and data were recorded; (3) The previous operation was repeated until the distance between the tag node and the base station node reached 3 m.

Based on the analysis of the obtained experimental data, the input signal characteristic RSSI was grouped into five fuzzy sets in this study, represented by “very large”, “large”, “medium”, “small” and “very small”. The input signal characteristic FPPL was classified into six fuzzy sets indicated by “very large”, “large”, “medium”, “small”, “very small” and “extremely small”. The input signal characteristic RT was assigned into five fuzzy sets expressed by “extremely small”, “very small”, “small”, “medium” and “large”. Moreover, the output NLOS error was divided into five fuzzy sets presented as “very small”, “small”, “medium”, “large” and “very large”. In this paper, a total of 25 fuzzy rules were formulated according to the collected data of the CIR signal characteristics RSSI, FPPL and RT of UWB and the NLOS errors, as well as the established fuzzy sets, as shown in Table 1.

Table 1. The fuzzy rules based on RSSI, FPPL and RT of UWB.

	RSSI	FPPL	RT	Range Error
1	very large	very large	extremely small	very small
2	very large	very large	very small	very small
3	very large	large	extremely small	very small
4	very large	large	very small	very small
5	very large	medium	extremely small	small
6	very large	small	large	small
7	large	very large	extremely small	small

Table 1. *Cont.*

	RSSI	FPPL	RT	Range Error
8	large	large	extremely small	small
9	large	large	very small	small
10	large	medium	small	small
11	large	extremely small	small	small
12	large	very small	small	small
13	large	very small	medium	medium
14	large	medium	extremely small	medium
15	large	medium	very small	medium
16	medium	small	small	medium
17	medium	small	medium	medium
18	very large	medium	small	large
19	very large	small	small	large
20	large	small	small	large
21	medium	very small	medium	large
22	small	small	small	large
23	small	small	large	large
24	very large	very small	large	very large
25	small	very small	large	very large

3. Adaptive Anti-NLOS Error KF Algorithm

3.1. KF Algorithm

Assuming that the distance between the tag node and the base station node changes uniformly in a short period, the motion state of the tag node could be expressed as $x(k) = [d(k) \ v(k)]^T$, where $d(k)$ represents the distance between the tag node and the base station at the moment k , and $v(k)$ refers to the speed of the tag node at the moment k . Moreover, $w(k - 1) = [w_d(k - 1) \ w_v(k - 1)]^T$ was applied to indicate that the tag is inevitably disrupted by the process noise during the motion, where $w_d(k - 1)$ stands for the process noise of range at the moment $k - 1$, and $w_v(k - 1)$ is the process noise of speed at the moment $k - 1$. Then, the system state can be expressed by Equation (4):

$$\begin{cases} d(k) = d(k - 1) + v(k - 1) \times T + w_d(k - 1) \\ v(k) = v(k - 1) + w_v(k - 1) \end{cases} \tag{4}$$

where T is the sampling time.

In this way, the KF model of the ranging data filtering was obtained, and Equations (5) and (6) stood for the state equation and the observation equation, respectively:

$$x_k = F_k x_{k-1} + w_{k-1} \tag{5}$$

$$z_k = H_k x_k + v_k \tag{6}$$

where F_k is the state transition matrix, and w_{k-1} means the process noise at the moment $k - 1$, obeying the Gaussian distribution with a mean value of 0 and a variance matrix of Q_{k-1} . In addition, H_k refers to the observation matrix, and v_k represents the observation noise at the moment k , which complies with the Gaussian distribution with a mean value of 0 and a variance matrix of R_k .

Assuming that the estimated state of KF at the moment $k - 1$ is \hat{x}_{k-1} , and the observed value of KF at the moment k is z_k , the estimated state \hat{x}_k calculation processes of KF at the moment k are as follows:

(1) One-step prediction

The estimated state \hat{x}_{k-1} of KF at the moment $k - 1$ was used to predict the state at the moment k . In other words, the observed value z_{k-1} at the moment $k - 1$ was applied to estimate the linear minimum variance of the actual state x_k . Furthermore, the least mean square error at the moment $k - 1$ was estimated via $\hat{x}_{k-1} = E\{x_{k-1}/z_{k-1}\}$, and w_{k-1} only affected the value of x_k . Therefore, the value of $E\{w_{k-1}/z_{k-1}\}$ was set to 0 to obtain the formula for one-step state prediction:

$$\begin{aligned} \hat{x}_{k|k-1} &= E\{x_k/z_{k-1}\} \\ &= F_k E\{x_{k-1}/z_{k-1}\} + E\{w_{k-1}/z_{k-1}\} = F_k \hat{x}_{k-1} \end{aligned} \tag{7}$$

(2) Covariance matrix of estimated errors

Supposing that the value of one-step state prediction is $\tilde{x}_{k|k-1}$, $\hat{x}_{k|k-1}$ means the observed value predicted by substituting $\hat{x}_{k|k-1}$ into the observation equation. In the framework of filtering theory, the error between the observed value predicted by $\tilde{z}_{k/k-1}$ and the actually observed value is called innovation. After appropriate weighting of $\tilde{z}_{k/k-1}$, $\tilde{x}_{k|k-1}$ information was obtained. Thus, the state after correction is estimated as follows:

$$\hat{x}_k = \hat{x}_{k|k-1} + K_k(z_k - H_k \hat{x}_{k|k-1}) \tag{8}$$

where K_k is the KF gain matrix.

The covariance matrix of the one-step prediction error is defined below:

$$P_{k|k-1} = E\left\{\tilde{x}_{k|k-1}\tilde{x}_{k|k-1}^T\right\} \tag{9}$$

With the known condition of $E\{v_k v_k^T\} = R_k$, where R_k indicates the variance of the observation noise, the estimated error was not correlated with the observation noise, that is, $E\left\{\tilde{x}_{k|k-1} v_k^T\right\} = E\left\{v_k \tilde{x}_{k|k-1}^T\right\} = 0$, which was substituted into Equation (9):

$$P_k = (I - K_k H_k) P_{k|k-1} (I - K_k H_k)^T + K_k R_k K_k^T \tag{10}$$

Through the analysis of the recursion formula from P_{k-1} to $P_{k|k-1}$, the estimated error at the moment $k - 1$ and the process noise at current moment k were not correlated either, namely, $E\left\{\tilde{x}_{k-1} w_k^T\right\} = 0$, so the covariance matrix of the one-step prediction error was acquired by substituting the formula into Equation (9):

$$P_{k|k-1} = F_k P_{k-1} F_k^T + Q_{k-1} \tag{11}$$

(3) Gain matrix K_k

To minimize the estimated error covariance P_k , the smallest trace of the matrix is usually adopted, that is

$$\frac{\partial}{\partial K_k} tr(P_k) = 0 \tag{12}$$

Equation (10) was substituted into Equation (12) to form the KF gain matrix:

$$K_k = P_{k|k-1} H_k^T (H_k P_{k|k-1} H_k^T + R_k)^{-1} \tag{13}$$

Then, Equation (13) was substituted into Equation (10) to simplify the covariance matrix of the estimated error:

$$P_k = (I - K_k H_k) P_{k|k-1} \tag{14}$$

3.2. Anti-NLOS KF Algorithm and Its Improvement

In actual UWB positioning, the measured range can be easily affected by the NLOS and multi-path effects, thus inducing abnormal points and leading to poor filtering performance, deviations and even converge failure. An anti-NLOS KF algorithm proposed in the literature [26] mainly compares the triple innovation variance with innovation to determine the existence of NLOS errors. If there are NLOS errors, they will be decreased by zooming in the innovation at a fixed ratio. The anti-NLOS KF algorithm is mainly illustrated below:

Assuming the innovation Δ_k and its variance matrix D_k at the moment k are expressed as Equation (15) and (16), respectively:

$$\Delta_k = z_k - H_k \hat{x}_{k/k-1} \tag{15}$$

$$D_k = E\{\Delta_k \Delta_k^T\} = H_k P_{k/k-1} H_k^T + R_k \tag{16}$$

According to the triple variance theory and combined with Equations (15) and (16), a method to determine whether a measured value is affected by NLOS can be obtained in Equation (17):

$$|\Delta_k^i| \leq 3\sqrt{D_k^i} \tag{17}$$

where D_k^i is the element i on the diagonal of matrix D_k , and Δ_k^i stands for the element i of Δ_k . If Equation (17) was not met, Equation (18) would be used to correct its innovation:

$$\Delta_k^i = \alpha \Delta_k^i, \alpha \in [0, 1] \tag{18}$$

where α is the correction factor of innovation.

It can be seen from the above algorithm that the inhibitory effect of the KF algorithm on the NLOS errors is mainly determined by the fixed correction factor of innovation. In an actual UWB mobile positioning scene, the NLOS changes. Hence, the fixed value of α has a limited inhibitory effect on the NLOS errors.

Based on the literature [27], an adaptive anti-NLOS KF algorithm was proposed in this paper, where the value of α was automatically adjusted as per the changes in the difference between innovation and innovation variance, so as to further improve the anti-NLOS error effect. The automatic adjustment method for α designed in this paper is expressed in Equation (19):

$$\begin{cases} \alpha = 1 - (\Delta_k^i / (3\sqrt{D_k^i}) - 1) \times b & , 3\sqrt{D_k^i} \leq \Delta_k^i \leq 6\sqrt{D_k^i} \\ \alpha = 1 - b & , \Delta_k^i > 6\sqrt{D_k^i} \end{cases} \tag{19}$$

where b is the maximum down-scaling ratio of the correction factor α , ranging from 0 to 1. This factor should not be too small. Otherwise, a large amount of information at the current moment will be lost, eventually remarkably lowering the filtering accuracy. As a result, several experiments are needed for adjustment when setting the value of b .

In the scene of UWB mobile positioning, the innovation changed as the influence of NLOS on ranging data was increased or decreased, and α , used to reduce innovation multiplication, varied between $1 - b$ and 1, thus achieving the anti-NLOS error effect through adaptive adjustment. The flow chart of the adaptive anti-NLOS KF algorithm is displayed in Figure 3.

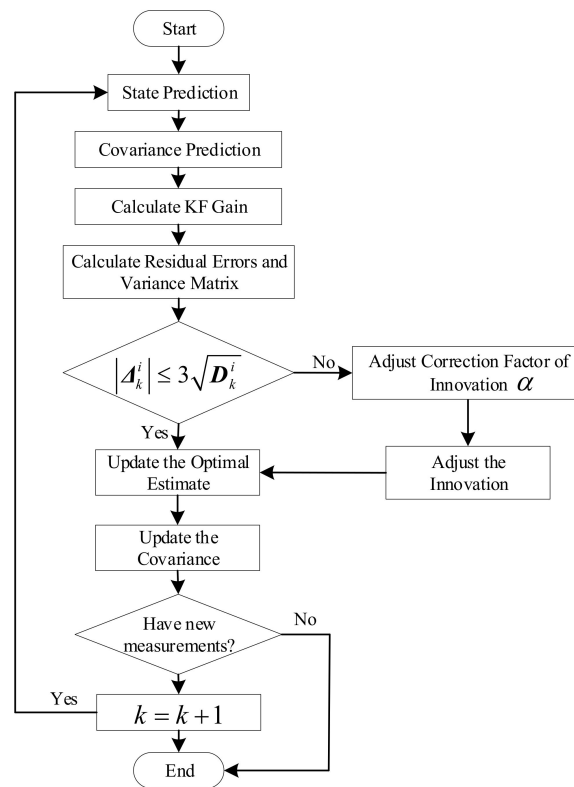


Figure 3. Flow chart of the adaptive anti-NLOS KF algorithm.

4. Positioning Algorithm Based on Fuzzy Inference and Adaptive Anti-NLOS KF

4.1. Adaptive Anti-NLOS KF Positioning Algorithm

The LS positioning algorithm has a small influence on the NLOS errors and strong robustness. In this paper, the adaptive anti-NLOS KF was combined with LS positioning, and an adaptive anti-NLOS KF positioning algorithm was proposed. In this algorithm, the adaptive anti-NLOS KF was first performed on the original ranging data to eliminate the NLOS errors therein. Then, the filtered ranging data were substituted into the LS positioning algorithm for the final estimation of the tag position. The flow chart of the adaptive anti-NLOS KF positioning algorithm is shown in Figure 4.

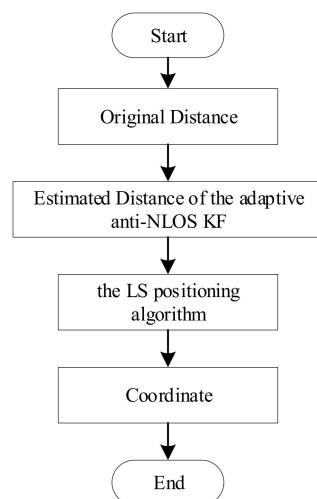


Figure 4. Flow chart of the adaptive anti-NLOS KF positioning algorithm.

4.2. Positioning Algorithm Combining Fuzzy Inference with Adaptive Anti-NLOS KF

The positioning algorithm based on fuzzy inference can estimate the NLOS ranging errors through the CIR signal characteristics, thereby improving the positioning accuracy. In the ranging error mitigation method for CIR signal characteristics based on fuzzy inference, however, the fuzzy rules are established by virtue of the data collected in a specific experimental environment, which fails to cover all situations in actual positioning. Additionally, when a fuzzy rule is established based on the data of one sampling point, the fuzzy estimation effect based on the data of other sampling points will be degraded, which usually cannot be altered by the supplementation or deletion of fuzzy rules. In contrast, the adaptive anti-NLOS KF positioning algorithm is able to identify the NLOS errors by comparing innovation with its variance and automatically adjusting the value of the correction factor of innovation on the basis of the changes in the difference between the innovation and its variance, thereby mitigating the NLOS errors. Nevertheless, the positioning accuracy of the adaptive anti-NLOS KF algorithm tends to decrease with the increasing influence of NLOS errors.

Based on the advantages and disadvantages of the two algorithms mentioned above, a positioning algorithm integrating fuzzy inference and adaptive anti-NLOS KF was put forward in this paper. The ranging error was estimated with fuzzy inference performed on the RSSI, FPPL and RT characteristics of the CIR signals collected during each range. Afterward, the collected original ranging data minus the ranging error obtained through fuzzification were regarded as the range data after fuzzy inference, which was subsequently substituted into the adaptive anti-NLOS KF algorithm as the observation value to obtain the final distance estimate. Last but not least, the final estimated range information was input into the LS positioning algorithm, so as to complete the position estimation of the tag nodes. The positioning algorithm combining fuzzy inference with adaptive anti-NLOS KF is illustrated in Figure 5.

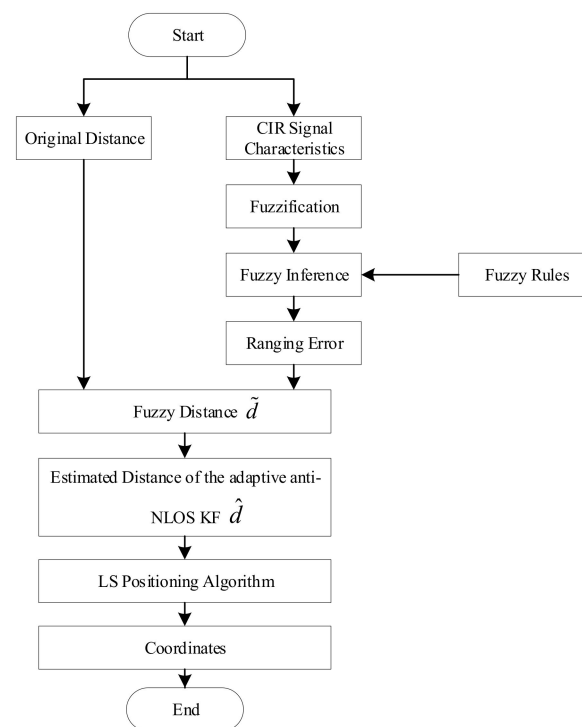


Figure 5. Flow chart of the positioning algorithm combining fuzzy inference with adaptive anti-NLOS KF.

5. Experimental Results and Analyses

5.1. Architecture of the Positioning Experiment System

The positioning experiment system designed in this paper consisted of a UWB positioning system and a host computer system. The UWB positioning system had four DWM1000 UWB positioning node modules manufactured by Big Bear Electric Technology Co., Ltd. (Guangzhou, China), as well as a moving vehicle. With STM32F103 as the master control, the DWM1000 modules supported serial communication and multi-tag positioning. The moving vehicle, controlled by an STM32 single-chip microcomputer, supported PS2 remote control, PID speed control and tracking. The measuring distance of the system equipment was about 10 m. The working procedure of the positioning experiment system is described below. The tag node initiated ranging communication in each base station, and then, the ranging data and the corresponding CIR signal characteristic data obtained from each base station were sent to the primary base station. Later, the primary base station gathered the data from all base stations and transmitted them to the host computer via the serial port. After that, data analysis and processing were conducted using the host computer system programed by the QT software, and the processed data were substituted into the designed algorithm modules to obtain highly accurate positioning data, which were eventually displayed on the interface in real time.

In this paper, static and dynamic positioning experiments were carried out in an actual NLOS environment to compare the positioning algorithm for NLOS error mitigation based on fuzzy inference, the adaptive anti-NLOS KF positioning algorithm and the positioning algorithm combining fuzzy inference with adaptive anti-NLOS KF, so as to verify the performance of the UWB positioning algorithm proposed.

5.2. Static Positioning Experiment

The static positioning experiment was performed in a rectangular region with a length of 200 cm and a width of 300 cm in the laboratory (Figure 6). The three base station nodes, numbered A_1 , A_2 and A_3 in a sequence, were placed at three corners of the rectangular region, corresponding to the coordinates (0, 0), (200, 0) and (0, 300), respectively. The iron plate obstacle was placed at (0, 68) and the wooden board obstacle at (0, 270). Finally, the tag nodes were placed sequentially at (50, 150), (50, 175), (50, 200), (75, 200) and (100, 200) for positioning testing.

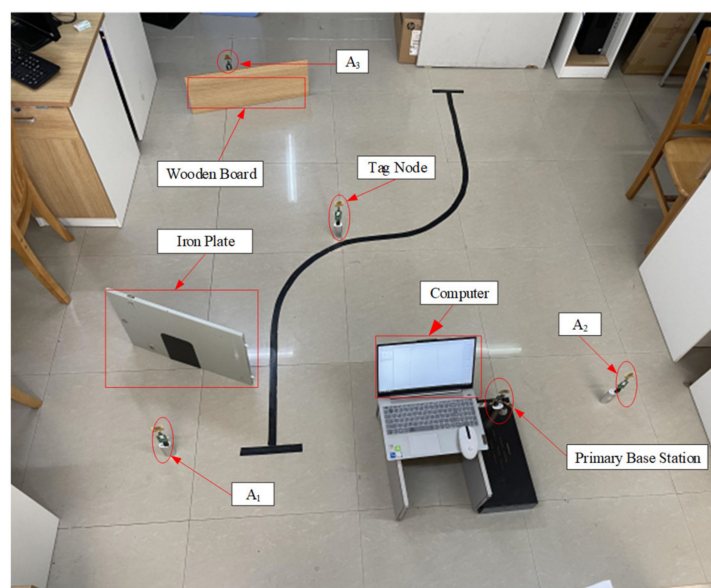


Figure 6. Environment of the static positioning experiment.

The settings of parameters of the positioning algorithm based on fuzzy inference and adaptive anti-NLOS KF and the adaptive anti-NLOS KF positioning algorithm are shown below [28]:

$$Q = \begin{bmatrix} 4 & 0 \\ 0 & 0.4 \end{bmatrix}, R = 10, T = 0.5, b = 0.25$$

Q is the process noise matrix, R is the observation noise matrix, T is the sampling time, b is the maximum reduction in the correction factor.

The positioning experiment system performed positioning every 0.5 s and closed the serial port whenever over 600 pieces of positioning data were collected. Then, the position of the tag nodes was adjusted for the positioning experiment at the next position until tests at all positioning points were completed. The static positioning data at the five testing points were analyzed to obtain the corresponding RMS errors (RMSEs) of the three algorithms (Table 2).

Table 2. RMSEs of static positioning under NLOS conditions.

Positioning Algorithm	(50, 150)	(50, 175)	(50, 200)	(75, 200)	(100, 200)
Adaptive Anti-NLOS KF Positioning Algorithm	21.5767	29.6724	28.3351	12.8494	29.5745
Fuzzy Inference Algorithm	15.5637	19.4664	28.5161	14.5265	16.7417
Positioning Algorithm Combining Fuzzy Inference with Adaptive Anti-NLOS KF	14.8205	19.1152	25.2317	12.8007	15.1546

As shown in Table 1, in the five positioning tests, the positioning algorithm combining fuzzy inference with adaptive anti-NLOS KF had the smallest RMSE; the fuzzy inference algorithm had four RMSEs less than 20 cm; and the adaptive anti-NLOS KF positioning algorithm had four RMSEs larger than 20 cm.

In order to more intuitively compare the performance of the three algorithms, the scatter diagram and cumulative distribution function (CDF) diagram were drawn to analyze the experimental data of the tag node at (50,150) (Figures 7 and 8, respectively).

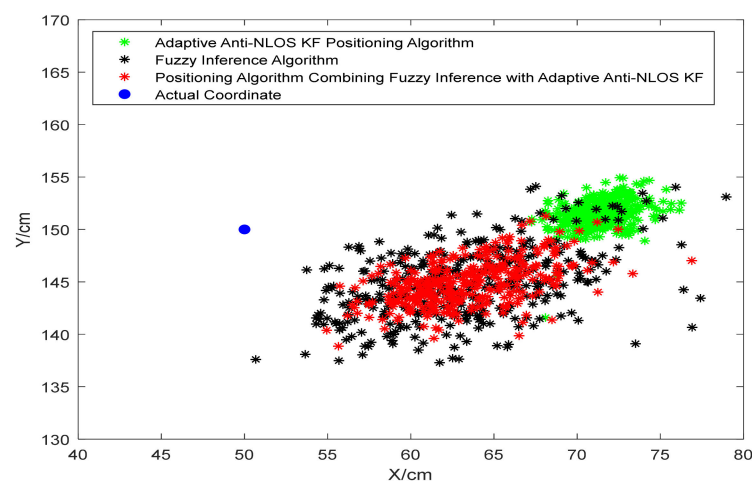


Figure 7. Scatter diagram of static positioning by three positioning algorithms.

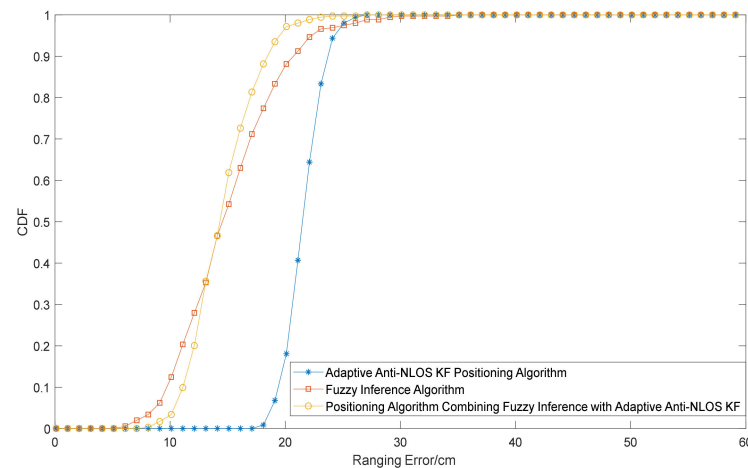


Figure 8. CDF diagram of the three positioning algorithms.

According to Figure 7, compared with those of the positioning algorithm based on fuzzy inference, the center of the scatter diagram of the positioning algorithm combining fuzzy inference with adaptive anti-NLOS KF was closer to the actual coordinate, and the scatter diagram was more concentrated. Therefore, before the integration of the positioning algorithm based on fuzzy inference with the adaptive anti-NLOS KF positioning algorithm, there might be a large deviation between the estimated NLOS error and the actual NLOS error in some cases, which was significantly improved after the integration. In Figure 8, the probability of producing an error range of less than 19.1 cm by the positioning algorithm combining fuzzy inference with adaptive anti-NLOS KF was 0.93; that of the positioning algorithm based on fuzzy inference was 0.83; and that of the adaptive anti-NLOS KF positioning algorithm was only 0.06.

5.3. Dynamic Positioning Experiment

For better dynamic positioning testing, vehicle tracking was used for the experiment in this paper. The parameters of the three algorithms were the same as those in the previous static experiment. The environment of the dynamic positioning experiment is exhibited in Figure 9. The black line was paved according to the preset trajectory, starting at (50, 50) and ending at (150, 249.7). The tag nodes were placed on a 4 cm high vehicle. Then, the actual measured distance between the UWB tag and UWB was calculated as $d = \sqrt{d_c^2 - (4)^2}$, where d_c is the measured distance. Next, the vehicle was located at (50, 50), and the primary base station node was connected with the host computer. In the end, two iron plate obstacles were placed at (11, 35) and (64, 240), respectively, and the wooden board obstacle was at (155, 75).

The vehicle moved at a constant speed along the black line in the experimental field, during which the system performed positioning once every 0.5 s, and data collection was stopped when the vehicle arrived at the endpoint. The dynamic positioning data were then analyzed to obtain the positioning trajectories of the three algorithms (Figure 10). The RMSE curves of the positioning trajectories are given in Figure 11, and the RMSEs of the three algorithms in X direction, Y direction and overall positioning are listed in Table 3.

According to Figures 10 and 11, the positioning trajectory of the positioning algorithm combining fuzzy inference with adaptive anti-NLOS KF was closer to the target trajectory in the second half, and its positioning RMSE was lower than that of the other two algorithms at most moments. These findings revealed that the combination of historical information and characteristic information of the CIR signals could better mitigate the NLOS errors.

It was manifested in Table 2 that the positioning accuracy of the positioning algorithm combining fuzzy inference with adaptive anti-NLOS KF was improved to varying degrees in comparison with that of the other two algorithms. In contrast with those of the adaptive anti-NLOS KF positioning algorithm, the RMSE was reduced by 48.83% in the X direction,

38.37% in the Y direction and 43.31% in overall positioning. Furthermore, compared with those of the positioning algorithm based on fuzzy inference, the RMSEs in the X direction, Y direction and overall positioning were lowered by 24.54%, 12.89% and 12.89%, respectively.

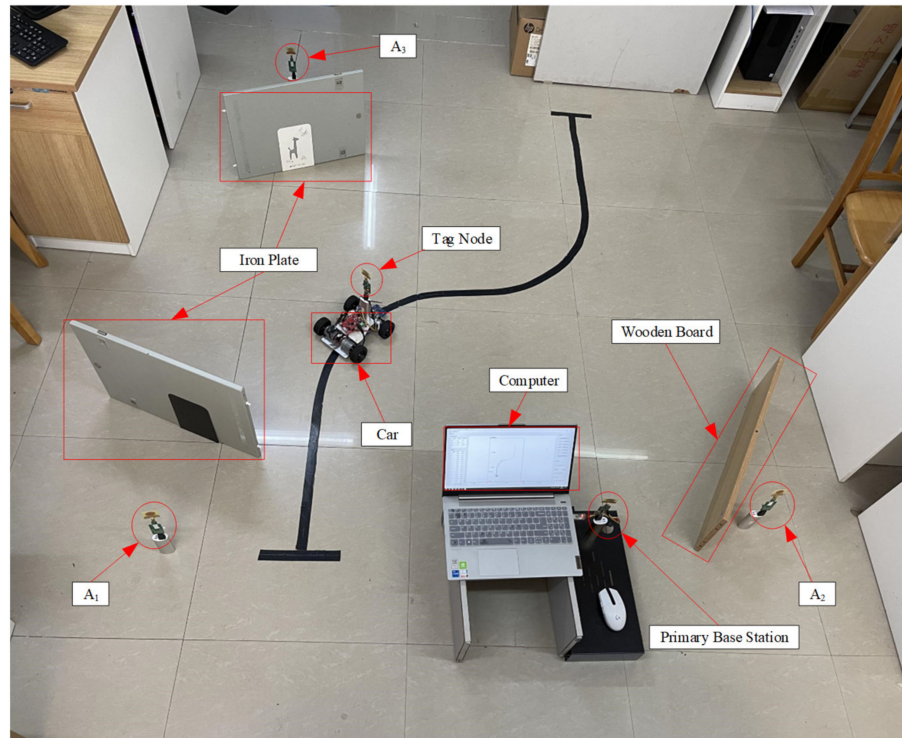


Figure 9. Environment of the dynamic positioning experiment.

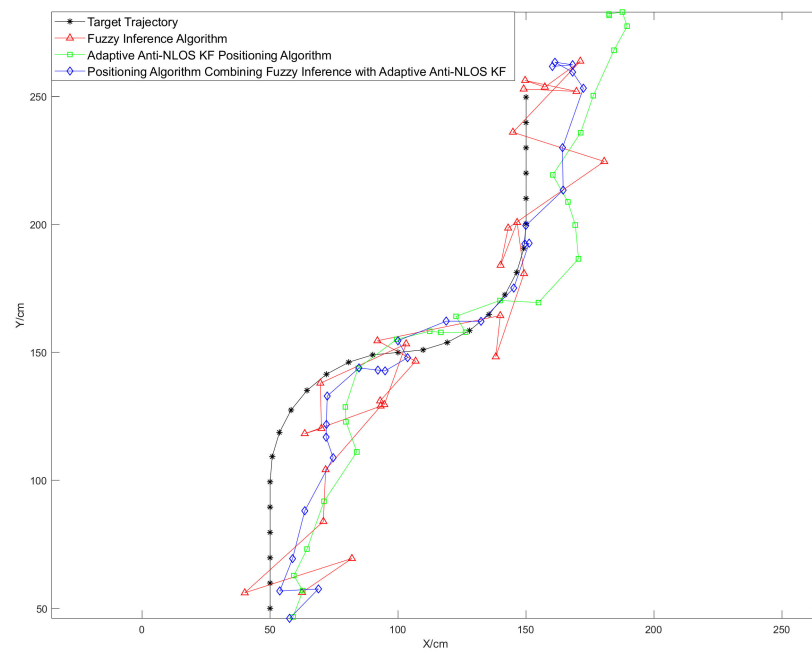


Figure 10. Positioning trajectories of the three algorithms.

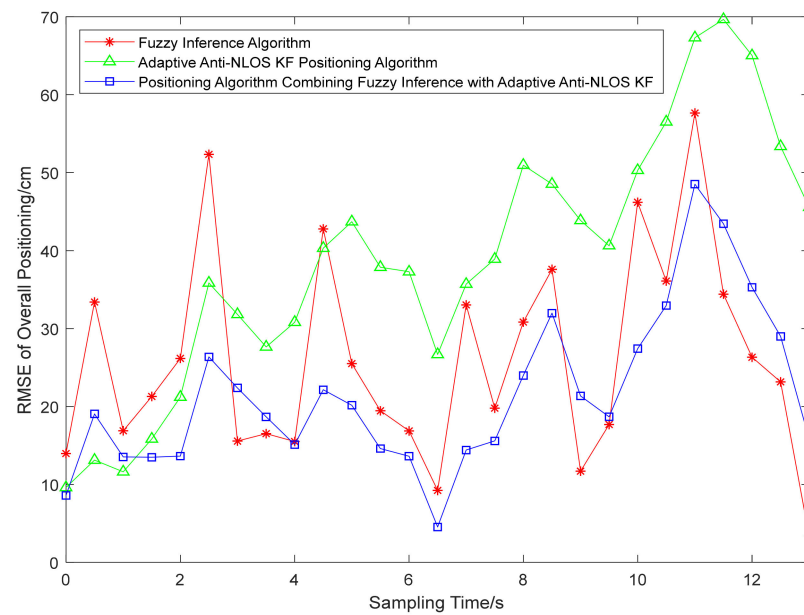


Figure 11. RMSE curves of the positioning trajectories.

Table 3. Mobile positioning of RMSEs in NLOS conditions.

Positioning Algorithm	X Direction RMSE (cm)	Y Direction RMSE (cm)	Overall Positioning RMSE (cm)
Adaptive Anti-NLOS KF Positioning Algorithm	29.6038	29.8749	42.0582
Fuzzy Inference Algorithm	20.0713	21.1351	29.1471
Positioning Algorithm Combining Fuzzy Inference with Adaptive Anti-NLOS KF	15.1454	18.4096	23.8390

6. Conclusions

- (1) In terms of the decreased positioning accuracy caused by the changes in NLOS errors due to UWB mobile node positioning, a UWB node positioning algorithm combining fuzzy inference with adaptive anti-NLOS KF was proposed in this paper. It classified the CIR signal characteristics by establishing fuzzy rules, adjusted the innovation value based on the change in the difference between the innovation and its variance in the KF algorithm, recognized and mitigated the NLOS errors and substituted the positioning estimation data into the LS positioning algorithm for node position estimation.
- (2) Static and dynamic experiments were conducted to verify the positioning algorithm based on fuzzy inference, the adaptive anti-NLOS KF positioning algorithm and the positioning algorithm combining fuzzy inference with adaptive anti-NLOS KF. In the static positioning experiment, the probability of producing an error range of less than 19.1 cm by the positioning algorithm combining fuzzy inference with adaptive anti-NLOS KF was 0.93, which was much better than the positioning algorithm based on fuzzy inference and the adaptive anti-NLOS KF positioning algorithm. In the dynamic positioning experiment, compared with the adaptive anti-NLOS KF positioning algorithm, the RMSE was reduced by 43.31% in overall positioning. Furthermore, compared with those of the positioning algorithm based on fuzzy inference, the RMSEs in overall positioning were lowered by 12.89%. The experimental

results demonstrated that the static positioning estimation and dynamic positioning trajectory of the positioning algorithm combining fuzzy inference with adaptive anti-NLOS KF were closer to the actual node position, the positioning performance was significantly improved, and the positioning accuracy was increased.

- (3) Because only three CIR signal characteristics (FPPL, RSSI and RT) were selected, the positioning accuracy of the positioning algorithm based on fuzzy inference might occasionally be significantly reduced. In the future, more CIR signal characteristics can be considered to improve the estimation accuracy of NLOS errors, thereby improving the positioning accuracy.

Author Contributions: Conceptualization, L.Z.; methodology, J.W. and Z.K.; software, Z.Z., J.W. and Z.K.; formal analysis, Z.Z. and S.Z.; data curation, S.Z.; writing—original draft preparation, J.W. and S.Z.; writing—review and editing, S.Z. and L.Z.; supervision, L.Z.; project administration, L.Z. All authors have read and agreed to the published version of the manuscript.

Funding: This work was supported by the National Natural Science Foundation of China (No. 61741303), the key laboratory of spatial information and geomatics (Guilin University of Technology) (No. 19-185-10-08), Scientific Research Basic Ability Improvement Project of Young and Middle-Aged Teachers in Colleges and Universities in Guangxi (No. 2021KY0260).

Institutional Review Board Statement: The article does not cover human research, so it does not cover this item.

Informed Consent Statement: Not applicable.

Data Availability Statement: Not applicable.

Conflicts of Interest: The authors declare no conflict of interest.

References

- Shi, D.Q.; Mi, H.Y.; Collins, E.G.; Wu, J. An Indoor Low-Cost and High-Accuracy Localization Approach for AGVs. *IEEE Access* **2020**, *8*, 50085–50090. [[CrossRef](#)]
- Zhou, N.; Lawrence, L.; Bai, R.B.; Terry, M. Novel prior position determination approaches in particle filter for ultra wideband (UWB)-based indoor positioning. *Navigation* **2021**, *68*, 277–292. [[CrossRef](#)]
- Typiak, R.; Rykała, Ł.; Typiak, A. Configuring a UWB Based Location System for a UGV Operating in a Follow-Me Scenario. *Energies* **2021**, *14*, 5517. [[CrossRef](#)]
- Su, M.; Yang, Y.; Jiang, J. BeiDou system satellite-induced pseudorange multipath bias mitigation based on different orbital characteristic for static applications. *IET Radar Sonar Navig.* **2019**, *14*, 242–251. [[CrossRef](#)]
- Ala'a, A.; Gabriel, W.; Moayad, A. Machine learning-based indoor localization and occupancy estimation using 5G ultra-dense networks. *Simul. Model. Pract. Theory* **2022**, *118*, 102543.
- Safar, M.A.; Halgurd, S.M. A Comprehensive Review of Indoor/Outdoor Localization Solutions in IoT era: Research Challenges and Future Perspectives. *Comput. Netw.* **2022**, *212*, 109041.
- Sun, J.; Shang, J.N.; Liu, X.H.; Xu, H.L.; Wu, F. An Improved Weighted KNN Location Algorithm Based on Fuzzy Reasoning. *Chin. J. Sens. Actuators* **2020**, *33*, 882–888.
- Li, Y. *Research on Indoor Location Method Based on UWB/INS Combination*; Harbin Engineering University: Harbin, China, 2019.
- Sandra, D.; Igor, S.; Milica, J.; Goran, L.D. Multi-algorithm UWB-based localization method for mixed LOS/NLOS environments. *Comput. Commun.* **2022**, *181*, 365–373.
- Zhang, B.; Chen, X.; Liao, Y.N.; Tian, Q. UWB/INS indoor positioning algorithm based on DL-LSTM. *Transducer Microsyst. Technol.* **2021**, *40*, 147–150.
- Tian, G.L.; Zhang, L.J.; Li, Z.Y. UWB/INS integrated location method based on improved robust Kalman filter and SVR. *Electron. Meas. Technol.* **2022**, *45*, 79–84.
- Hu, Q.; He, T.J.; Jia, T.; Li, H.; Tang, Y.J. UWB/GPS combination positioning method. *J. Nanjing Univ. Sci. Technol.* **2018**, *42*, 76–81.
- Zhang, C.C. *Research on Indoor Combined Positioning Based on Wi-Fi/UWB/Barometer*; Southeast University: Nanjing, China, 2018.
- Liang, Y.; Zhang, Q.D.; Zhao, N.; Li, C.M. Indoor location method based on UWB and inertial navigation fusion. *Infrared Laser Eng.* **2021**, *50*, 293–306.
- Zhang, G.L.; Deng, Z.L.; Wen, L.; Ke, H.; Jiao, J.C. An UWB location algorithm for indoor NLOS environment. In Proceedings of the 2018 Ubiquitous Positioning, Indoor Navigation and Location-Based Services (UPINLBS), Wuhan, China, 22–23 March 2018; pp. 1–6.
- Liu, T.; Xu, A.; Sui, X. Adaptive Robust Kalman Filtering for UWB Indoor Positioning. *Chin. J. Sens. Actuators.* **2018**, *31*, 567–572.

17. Huang, B.; Li, W. Location Algorithm Based on Particle Filtering and Maximum Likelihood for TDOA under LOS_NLOS Conditions. *Comput. Simul.* **2022**, *39*, 481–489.
18. Chen, H.; Wang, G.; Ansari, N. Improved robust TOA-based localization via NLOS balancing parameter estimation. *IEEE Trans. Veh. Technol.* **2019**, *68*, 6177–6181. [[CrossRef](#)]
19. Barral, V.; Escudero, C.J.; García-Naya, J.A. NLOS classification based on RSS and ranging statistics obtained from low-cost UWB devices. In Proceedings of the 2019 27th European Signal Processing Conference (EUSIPCO), A Coruña, Spain, 2–6 September 2019; pp. 1–5.
20. Stefano, M.; Wesley, M.G.; Henk, W.; Moe, Z.W. NLOS identification and mitigation for localization based on UWB experimental data. *IEEE J. Sel. Areas Commun.* **2010**, *28*, 1026–1035.
21. Yang, X. NLOS mitigation for UWB localization based on sparse pseudo-input Gaussian process. *IEEE Sens. J.* **2018**, *18*, 4311–4316. [[CrossRef](#)]
22. Sunil, K.M.; Muhammad, A.; Farooq, A.; Kemal, T. Empirical Based Ranging Error Mitigation in IR-UWB: A Fuzzy Approach. *IEEE Access* **2019**, *7*, 33686–33697.
23. Che, F.; Ahmed, Q.Z.; Khan, F.A.; Lazaridis, P.I. Anomaly Detection Based on Generalized Gaussian Distribution approach for Ultra-Wideband (UWB) Indoor Positioning System. In Proceedings of the 2021 26th International Conference on Automation and Computing (ICAC), Portsmouth, UK, 2–4 September 2021; pp. 1–5.
24. Wang, C.Y.; Wang, J.; Ning, Y.P.; Yu, H. Study of noise reduction method for ultra wideband positioning. *Sci. Surv. Mapp.* **2019**, *44*, 175–181.
25. Yu, K.G.; Wen, K.; Li, Y.B.; Zhang, S.; Zhang, K.F. A novel NLOS mitigation algorithm for UWB localization in harsh indoor environments. *IEEE Trans. Veh. Technol.* **2018**, *68*, 686–699. [[CrossRef](#)]
26. Jia, Y.W.; Duan, X.; Zhang, H.M.; Duan, T.Y.; Xu, Q.G.; Mao, H. Design optimization method of Mamdini type fuzzy controller applied to research reactor. *At. Energy Sci. Technol.* **2021**, *55*, 1091.
27. Ge, L. *Research on High Precision Indoor Location and Clock Synchronization Algorithms Based on UWB*; Beijing University of Posts and Telecommunications: Beijing, China, 2019.
28. Li, J.Y. *Design and Implementation of RSSI Indoor Positioning Tracking Algorithm Based on Adaptive Kalman Filter*; Southeast University: Nanjing, China, 2019.